

1 Measurement of methane flux over an evergreen coniferous forest canopy using a relaxed eddy
2 accumulation system with tuneable diode laser spectroscopy detection

3

4 Corresponding author: Ayaka Sakabe,

5 e-mail address: sakabea@kais.kyoto-u.ac.jp

6 Tel.: 81-75-753-6149

7 Fax: and fax numbers: 81-75-753-6149

8

9

10 Ayaka Sakabe,¹ Ken Hamotani,² Yoshiko Kosugi,¹ Masahito Ueyama,² Kenshi Takahashi,³ Akito

11 Kanazawa,¹ Masayuki Itoh⁴

12 ¹Laboratory of Forest Hydrology, Graduate School of Agriculture, Kyoto University, Kitashirakawa

13 Oiwake-cho, Sakyo-ku, Kyoto 606-8502, Japan

14 ² School of Life and Environmental Sciences, Osaka Prefecture University, Gakuen-cho 1-1, Sakai,

15 599-8531, Japan

16 ³ Research Institute for Sustainable Humanosphere, Kyoto University, Gokasho, Uji , 611-0011, Japan

17 ⁴Center for Ecological Research, Kyoto University, Hirano, Otsu, 520-2113, Japan

18

19

20 **Abstract**

21 Very few studies have conducted long-term observations of methane (CH₄) flux over forest canopies. In
22 this study, we continuously measured CH₄ fluxes over an evergreen coniferous (Japanese cypress) forest
23 canopy throughout 1 year, using a micrometeorological relaxed eddy accumulation (REA) system with
24 tuneable diode laser spectroscopy (TDLS) detection. The Japanese cypress forest, which is a common
25 forest type in warm-temperate Asian monsoon regions with a wet summer, switched seasonally between a
26 sink and source of CH₄ probably because of competition by methanogens and methanotrophs, which are
27 both influenced by soil conditions (e.g., soil temperature and soil moisture). At hourly to daily timescales,
28 the CH₄ fluxes were sensitive to rainfall, probably because CH₄ emission increased and/or absorption
29 decreased during and after rainfall. The observed canopy-scale fluxes showed complex behaviours
30 beyond those expected from previous plot-scale measurements and the CH₄ fluxes changed from sink to
31 source and *vice versa*.

32

33 **1. Introduction**

34 Most research on methane (CH₄) fluxes from natural ecosystems has focused on wetlands or rice
35 paddy fields, which are thought to be large CH₄ sources and thus important components of the global CH₄
36 budget. Considering that a major portion of forest soil is water-unsaturated, forests are generally assumed

37 to be an insignificant atmospheric CH₄ sink, representing to about 6% of the global sink (Le Mer and
38 Roger 2001). However, studies have revealed that forest ecosystems, especially in wet warm climates, are
39 not always CH₄ sinks. For example, some upland soils could be a CH₄ source when soils become
40 water-saturated following precipitation events (Silver et al. 1999; Savage et al. 1997; van den Pol-van
41 Dasselaar et al. 1998). Wang and Bettany (1997) also reported that upland soils that were incubated
42 anaerobically began producing CH₄ within days or weeks. However, the CH₄ dynamics in whole forest
43 ecosystems are still poorly understood because of insufficient information on topographically complex
44 landscapes. It is important to quantify CH₄ fluxes in forest ecosystems because they cover a large portion
45 of continental areas.

46 Long-term CH₄ flux measurements in forested areas have been mostly performed using chamber
47 methods. While chamber methods are useful for understanding the processes controlling CH₄ fluxes on
48 small spatial scales (usually less than 1 m²), the small footprint of the measurement creates a difficult
49 scaling problem (Denmead 1994) when estimating landscape-scale fluxes in heterogeneous terrain such
50 as forests. Moreover, the occasional measurements of manual chambers restrict the time resolution. These
51 inherent limitations of chamber methods have made it difficult to evaluate CH₄ dynamics in whole forest
52 ecosystems, as CH₄ fluxes from forest soils have wide spatial and temporal variations. CH₄ fluxes in
53 forest ecosystems could have wide-ranging spatio-temporal variations both emission and absorption sides,
54 especially in the forest ecosystems which have wide spatio-temporal range in soil water status, such as

55 Asian monsoon forests under warm and humid climate, or boreal and tropical peat forests. Scaling up of
56 CH₄ fluxes in those types of forests and understanding CH₄ dynamics as a whole ecosystem would be
57 difficult only with chamber methods. In addition, both open and closed chambers disturb natural
58 environmental conditions during the measurement by affecting airflow, radiant energy receipt, and energy
59 transfer to the atmosphere (Denmead 1994). Consequently, CH₄ exchanges estimated by the chamber
60 method could contain biases and uncertainties if up-scaled to stand, watershed, and regional scales.

61 Micrometeorological methods such as the eddy covariance (EC) method are ideally suited for
62 continuous canopy-scale flux measurements integrated over a larger area without artificial disturbance.
63 Although the EC method has been widely used for canopy-scale flux measurements, it has not been used
64 until very recently for CH₄ measurements because it requires a fast-response and high-precision gas
65 analyzer. Recent technological advances in the application of tuneable diode laser spectroscopy (TDLS)
66 to *in situ* field measurements open the possibility of long-term EC measurement of CH₄ in a variety of
67 ecosystems. Previously, a limited number of CH₄ EC measurements have been obtained in peatlands
68 (Hendriks et al. 2008; Schrier-Uijl et al. 2009), rice paddy fields (Simpson et al. 1994), and prairies (Kim
69 et al. 1998a, b). The lack of long-term CH₄ flux observations in forest ecosystems restricts our
70 understanding of canopy-scale CH₄ dynamics. However, measuring CH₄ exchange over forest ecosystems
71 is still challenging compared to measurements in the above source areas because of the small fluxes in
72 forests (Smeets et al. 2009). According to previous EC measurements in wetlands and farmlands, the

73 precision of the CH₄ concentration measurements was 2.9 ppb at 10 Hz using a Quantum Cascade Laser
74 Spectroscopy (QCLS) analyzer (QCL-TILDAS-76; Aerodyne Research Inc., Billerica MA, USA) (Kroon
75 et al. 2007). Recently, the open path sensor is available for the CH₄ EC measurement with the precision of
76 < 5 ppb at 10 Hz (McDermitt et al. 2011). However, those precisions are still insufficient to measure
77 small CH₄ fluxes at forest ecosystems if the CH₄ fluxes measured by chamber techniques (Itoh et al. 2005,
78 2007, 2009) assumed to be representative to the canopy scale exchange.

79 Although the state-of-the-art CH₄ analyzers could be insufficient for the EC measurements, those
80 analyzers are available for CH₄ flux measurements by using a micrometeorological relaxed eddy
81 accumulation (REA) method (Businger and Oncley 1990; Hamotani et al. 1996, 2001). The REA method
82 can take longer time for CH₄ concentration measurements, thus a laser signal can be averaged to optimize
83 the instrumental sensitivity, and higher precision of TDLS CH₄ analyzer was achievable. The flux,
84 calculated by the REA method, is equal to the difference in the mean concentrations of the trace gas of
85 interest associated with updraft and downdraft, multiplied by the standard deviation of the vertical wind
86 velocity and an empirical coefficient.

87 In this study, we employed an REA method (Businger and Oncley 1990; Hamotani et al. 1996, 2001)
88 with a TDLS CH₄ analyzer for long-term observation of CH₄ fluxes from a temperate evergreen
89 coniferous forest site. Our goal was to examine whether the REA method is applicable to (1) measure
90 CH₄ fluxes over the forest canopy, (2) reveal the amplitude and seasonal variations in CH₄ fluxes, and (3)

91 examine the response of CH₄ fluxes to rainfall. This is the first report showing the seasonal cycle of
92 canopy-scale CH₄ fluxes in a temperate forest.

93

94 **2. Methods**

95 **2.1 Site description**

96 The observations were made in a coniferous forest in the Kiryu Experimental Watershed, (KEW; area:
97 5.99 ha) in Shiga Prefecture, Japan. A meteorological observation tower is located in a small catchment
98 within KEW (Fig. 1). The forest consists of 50-year-old Japanese cypress (*Chamaecyparis obtusa* Sieb. et
99 Zucc.). Mean tree height was approximately 16.8 m in 2007. The annual mean air temperature and
100 precipitation measured at the meteorological station shown in Fig. 1 from 2002 to 2009 were 13.3°C and
101 1,576 mm yr⁻¹, respectively. The site has a warm temperate monsoon climate with a wet summer. Rainfall
102 occurs throughout the year with two peaks in summer due to the Asian monsoon; the early summer ‘Baiu’
103 front season and the late summer typhoon seasons. The entire watershed is underlain by weathered granite
104 with considerable amounts of albite.

105 Canopy fluxes of heat, water, and CO₂ have also been measured at this site at 29-m above the ground,
106 using the EC method (e.g., Takanashi et al. 2005; Kosugi et al. 2007; Kosugi and Katsuyama 2007;
107 Ohkubo et al. 2007). Takanashi et al. (2005) reported that the CO₂ flux for 92% of the daytime flux and
108 81% of the nighttime flux originated from the forest area according to an analytical footprint model by

109 Schuepp et al. (1990). The trend in wind direction at this site did not change seasonally but had diurnal
110 variations. The daytime wind direction was from all directions, whereas the night-time wind direction was
111 mainly from the south (Kosugi et al. 2007). Some wetlands were located in riparian zones along streams
112 within the flux footprint area, which were either always submerged or periodically submerged. The
113 streams and the main wetland areas (approximately 10^0 - 10^2 m²) are shown in Fig. 1. The riparian zones
114 and wetlands were distributed in both the north and south directions within the flux footprint area. The
115 size of these areas could slightly increase after rainfall. Notably, an express highway was opened
116 approximately 400 m south of the tower in February of 2008. During night-time, this highway was always
117 inside of the flux footprint. The paddy fields were situated several km north to west of the tower, although
118 these area were mostly out of the flux footprint (Takanashi et al. 2005). CH₄ fluxes from wetlands and
119 water-unsaturated soils were investigated using a chamber method with a gas chromatograph analyzer
120 (Itoh et al. 2005, 2007, 2009). Comparisons of the CH₄ fluxes from the previous chamber data and the
121 present REA data will be described later.

122

123 **2.2. Measurements**

124 The CH₄ flux was measured using the REA method (Businger and Oncley 1990; Hamotani et al. 1996,
125 2001). Although the REA method is theoretically the same as the EC method, it does not require a fast
126 response from the gas analyzer compared to the EC method. Compared to wetlands, forest canopies are

127 more challenging sites for conducting CH₄ flux measurements by the EC method. This is because the
128 emission and absorption of CH₄ are both relatively small over forest canopies, and TDLS analyzers may
129 not always be precise enough to detect the fluxes. The greatest benefit of applying the REA method is that
130 sufficient precision in CH₄ concentration TDLS measurements is achievable by signal averaging over a
131 longer duration. The precision of the TDLS CH₄ analyzer (FMA-200; Los Gatos Research, Mountain
132 View, CA, USA) is 3 ppb at 10 Hz rate, 1 ppb at 1 Hz rate and 0.1 ppb at 100 s rate according to the
133 catalog specifications. Moreover, the REA method can save electronic consumption and minimize the
134 possible noises induced by the pressure drift of the measurement cell of the TDLS CH₄ analyzer, because
135 the REA method with lower sampling frequency can measure CH₄ fluxes without a high-power vacuum
136 pump. The another advantage of the REA method is that it does not require any corrections such as high
137 frequency attenuation for closed-path EC method or WPL correction (Webb et al. 1980) for open-path EC
138 methods, which could obscure the observed small flux values at the forest ecosystems. One possible
139 disadvantage of the REA method involves the switching speed of the valve system, which may lead to the
140 loss of high frequency information, however those effects can be negligible at measurements over tall
141 forest canopies, such as in our forest (Ueyama et al. 2009). Equation 1 expresses CH₄ flux (F_{CH_4} , nmol
142 m⁻² s⁻¹ (Subsequently, we use this abbreviation only for CH₄ flux measured by the REA method). This
143 equation can also be used to calculate CO₂ flux (F_{CO_2} , μmol m⁻² s⁻¹):

144

145
$$F_{CH_4} = \sigma_w \left(\overline{S_{CH_4}^+} - \overline{S_{CH_4}^-} \right) \rho_a b \quad (1)$$

146

147 where σ_w is the standard deviation (SD) of the vertical wind velocity (w , m s⁻¹), $\overline{S_{CH_4}^+}$ and $\overline{S_{CH_4}^-}$
 148 are the 30-minute mean CH₄ mole fractions (ppmv) associated with updraft and downdraft, respectively,
 149 and ρ_a (mol m⁻³) is molar air density. The coefficient b was empirically determined from EC data using air
 150 temperature given by Eq. 2:

151

152
$$b = \frac{\overline{w'T'}}{\sigma_w \left(\overline{T^+} - \overline{T^-} \right)} \quad (2)$$

153

154 where $\overline{T^+}$ and $\overline{T^-}$ are 30-min mean fast-response temperature data associated with updraft and
 155 downdraft, respectively. We determined b to be 0.59, which is the average of 16,576 values obtained from
 156 Eq. 2 and the standard error was 0.04. The sensible heat flux and air temperature data used here was all
 157 data measured from August 2009 to August 2010 by the sonic anemometer (SAT-550; Kaijo Corp., Tokyo,
 158 Japan) mounted on top of the 29-m-tall tower. The term b was applied to both F_{CO_2} and F_{CH_4} . The value of
 159 b is relatively constant over a wide range of atmospheric stability (Bowling et al. 1998).

160

161

162

Our REA system consists of a sonic anemometer (SAT-550; Kaijo Corp.) to measure wind speed and
 direction, two diaphragm pumps (CV-201, Enomoto Co., Tokyo, Japan), four reservoirs (CCK-20; GL
 Science, Tokyo, Japan) to accumulate sampled gas, a CO₂/H₂O gas analyzer (LI-840; Li-Cor Inc., Lincoln,

163 NE, USA), a CH₄ gas analyzer (Baer et al. 2002; Hendriks et al. 2008) (FMA-200; Los Gatos Research)
164 and a data logger (CR1000; Campbell Scientific, Logan, UT, USA). The sonic anemometer was mounted
165 on top of the 29-m-tall tower and the air inlets were set directly below the sonic anemometer. Air samples
166 for updraft and downdraft were pulled through DK tubes (inner tube: 4 mm in diameter and coated with
167 aluminium) to the reservoirs by two diaphragm pumps at a constant flow rate (0.7 l min⁻¹). The frequency
168 of switching the pumps was 10 Hz. One pump worked only for updraft and the other worked only for
169 downdraft. Updraft or downdraft was determined by the difference between the instantaneous and
170 adjacent 15-min moving average of w . Air flow was switched using the solenoid valves (CKD
171 USB3-6-3-E; CKD Corp., Aichi, Japan) and controlled by the CR1000 data logger. To sequentially
172 determine the flux every half hour, we prepared two sets of sampling reservoirs: one pair of reservoirs
173 accumulated air during 0–30 min and the other pair accumulated air for the next 30–60 min. After
174 accumulating in the reservoirs for 30 min, the air in the reservoirs was pulled a diaphragm pump into the
175 CH₄ analyzer at a flow rate of approximately 0.7 l min⁻¹, and the air in each reservoir was analyzed for 2
176 min. Three filters were inserted in the gas sample line to protect the CH₄ analyzer from dust and insects.
177 Before entering the CO₂/H₂O and the CH₄ analyzers, the sampled air was dried using a gas dryer
178 (PD-50T-48; Perma Pure Inc., Toms River, NJ, USA). Dilution by water vapour, which could not be
179 completely removed by the drying system, was corrected for using the H₂O concentration measured with
180 the CO₂/H₂O analyzer. We confirmed that the gas dryer did not alter the CH₄ mixing ratio within

181 measurement uncertainties. Data were recorded at 10 Hz by the CR1000 data logger and stored on a
182 compact flash card using a compact flash module (CFM100, Campbell Scientific). A 10-s moving average
183 filtered the high frequency noises for the CO₂/H₂O analyzer and a 1-s moving average was used for the
184 CH₄ analyzer. Volumetric soil water content (VSWC) at a depth of 0–30 cm was measured with a CS616
185 water content reflectometer (Campbell Scientific) at four different points around the tower on the
186 water-unsaturated forest floor, and soil temperatures were measured with a thermistor (RT-10,11,12;
187 ESPEC Mic Corp., Kanagawa, Japan) at depths of 2 cm near the tower. Precipitation was measured with a
188 tipping bucket rain gauge at an open screen site near the tower. Air temperature above the canopy was
189 measured with a ventilated temperature and humidity sensor (HHP45AC; Vaisala, Helsinki, Finland) at a
190 height of 29 m above the ground.

191 In this study, we compared CO₂ fluxes measured by the REA and EC methods in order to examine the
192 validity of our REA system. An open-path CO₂/H₂O analyzer (LI-7500; Li-Cor) was used to measure CO₂
193 flux by the EC method. The double-rotation method was applied to the sonic anemometer velocities
194 (McMillen 1988), and the Webb, Pearman, Leuning (WPL) correction for the effect of air density
195 fluctuations (Webb et al. 1980) was applied to CO₂ flux using the EC method. Details of the EC
196 measurements have been described by Kosugi et al. (2007) and Okubo et al. (2007b).

197

198 **2.3. Data analysis**

199 Hendriks et al. (2008) described the specifications of the CH₄ analyzer used in this study in detail. To
200 examine the accuracy and precision of our CH₄ analyzer, calibration experiments were performed on site
201 using a standard CH₄ gas cylinder (Takachiho, Tokyo, Japan, 1773 ppb CH₄ in synthetic air) several times
202 during the course of this study. The typical SD for determining the CH₄ mixing ratio was 0.4 ppb with a
203 30-s moving average within a 3-min standard gas flow period, which is the same condition used for
204 calculating the reservoirs concentrations with the REA method; the reservoir concentrations were
205 averaged for 30 s and analyzed within 2 min. No significant drift in the measurement accuracy of the CH₄
206 analyzer was observed during the entire observation period (less than 6 ppb). We also examined the
207 detection limit of CO₂ and CH₄ fluxes in our REA system by storing the same air in reservoir pairs and
208 measuring the concentration difference in each pair. This check mode was performed during 1 day of
209 every month.

210 We performed a *t*-test (significance level: 0.05) for the CH₄ concentration difference between updraft
211 and downdraft to examine whether there was a statistical difference between the mean values. F_{CH_4}
212 assumed to be zero by the *t*-test (21.8% of all available data) is shown as grey circles in Figs. 3 and 5. All
213 CO₂ and CH₄ fluxes collected with the REA method were rejected when CO₂ flux data collected with the
214 EC method did not meet the stationary criteria (Foken and Wichur 1996; Aubinet et al. 2000). We also
215 rejected CO₂ and CH₄ fluxes collected during night-time under highly stratified conditions, using a
216 previously examined friction velocity threshold of 0.3 m s⁻¹ for the CO₂ flux data (Takanashi et al. 2005).

217 The total amount of F_{CH_4} data rejected by these criteria accounted for 66% of the entire data series.

218 The data analyzed in this study were recorded between 1 August 2009 and 31 August 2010. Data were
219 missing from 11 to 20 August 2009, from 16 June to 22 July 2010, and from 10 December 2009 to 17
220 February 2010 due to instrumental malfunctions.

221

222 **3. Results**

223 **3.1. Validity of the CH₄ fluxes collected with the REA system**

224 Before application to F_{CH_4} measurement, we validated our REA system by comparing F_{CO_2} measured
225 by the EC and REA method for daytime (Fig. 2a) and nighttime periods (Fig. 2b). The CO_2 fluxes by the
226 EC and REA methods were highly correlated for both daytime with a slope of 0.95, $r^2 = 0.72$ and the root
227 mean square error (RMSE) of $3.7 \mu\text{mol m}^{-2} \text{s}^{-1}$ (Fig. 2a) and nighttime with a slope of 0.81, $r^2 = 0.45$ and
228 the RMSE of $3.4 \mu\text{mol m}^{-2} \text{s}^{-1}$ (Fig. 2b). Although the slopes of the linear regression showed a slightly
229 smaller value than 1.0, the observed data both in the daytime and nighttime were mostly scattered around
230 the 1:1 line and the F_{CO_2} measured by the REA method did not show obviously higher or lower values
231 than those by the EC method (Fig. 2a, b). The F_{CO_2} measured by the EC and the REA methods had worse
232 correlation in the night-time than daytime (Fig. 2b).

233 The F_{CH_4} detection limit obtained from the check mode with our REA system showed a diurnal
234 variation because it depended on turbulent intensity (i.e., σ_w in Eq. 1 is larger in the daytime than in the

235 night-time) The night-time (0:00–6:00 and 18:00–24:00) and daytime (6:00–18:00) F_{CH_4} detection limits
236 averaged for all 14 check mode days were 4.2 ± 3.7 and 7.4 ± 5.9 $\text{nmol m}^{-2} \text{s}^{-1}$, respectively, and the
237 detection limits did not change seasonally.

238

239 **3.2. Amplitude and seasonal variations in CH_4 flux and its response to rainfall**

240 Figure. 3 shows the seasonal variations in (a) instantaneous F_{CH_4} , (b) air and soil temperature, and (c)
241 precipitation and VSWC. The average and SD of F_{CH_4} was 5.9 ± 11.5 $\text{nmol m}^{-2} \text{s}^{-1}$ for the summer of 2009
242 (August and September), 5.3 ± 10.4 $\text{nmol m}^{-2} \text{s}^{-1}$ for the fall of 2009 (October and November), 2.2 ± 10.9
243 $\text{nmol m}^{-2} \text{s}^{-1}$ for the winter of 2009 (December, February, and March), -10.0 ± 14.3 $\text{nmol m}^{-2} \text{s}^{-1}$ for the
244 spring of 2010 (April, May, and June), and -4.7 ± 15.3 $\text{nmol m}^{-2} \text{s}^{-1}$ for the summer of 2010 (July and
245 August). This site had a heterogeneous topography, and some riparian zones and wetlands were
246 distributed both in the north and south directions within the flux footprint area. However, the wind
247 direction at this site did not change seasonally. We confirmed that both daytime and night-time F_{CH_4} from
248 the north or south was not particularly larger than those from other wind directions by analysing F_{CH_4} for
249 each wind direction (Fig. 4). F_{CH_4} seasonally shifted from emission in the summer and fall of 2009 to
250 absorption in the spring of 2010. Then the absorption weakened and changed to emission in the summer
251 of 2010 (Fig. 3a). The diurnal patterns changed seasonally. In the summer and fall of 2009, F_{CH_4} showed
252 clear diurnal variation with an emission peak around noon (Figs. 5a, b and 6a, b). Large emission was

253 observed in the fall of 2009 during sequential rain events for several days (Fig. 5b). The emission
254 decreased with a decrease in air temperature (Fig. 6a, b), and then F_{CH_4} became almost zero in winter
255 (Figs. 5c and 6c). F_{CH_4} remained relatively small until the spring of 2010 (Fig. 5d). Then, F_{CH_4} gradually
256 shifted to exhibit a clear diurnal variation with an absorption peak around noon, which was an opposite
257 pattern compared to the previous summer (Fig. 5e and 6d). The magnitude of peak CH_4 absorption
258 increased with air temperature. Maximum CH_4 absorption was observed in June, when the absence of rain
259 lasted 17 days and VSWC decreased. After intense rainfalls in late July 2010, the CH_4 absorption rate
260 gradually decreased and seemed to shift to emission.

261 We detected evidence for short-term F_{CH_4} that rainfall was an important factor contributing to
262 increased CH_4 emission. After rainfall on 12 September 2009, high F_{CH_4} was observed on 13 September
263 2009 (Fig. 5a) and similarly on 27 October and 2 November 2009 (Fig. 5b). Averaged diurnal variations
264 for the summer of 2009 (August and September) and the fall of 2009 (October and November) also
265 showed that CH_4 emission increased after precipitation (Fig. 6a, b). Even when high CH_4 absorption rates
266 were observed around noon, rainfall contributed to weakening CH_4 absorption and/or F_{CH_4} switched to
267 emission as shown on 24 May 2010 (Fig. 5e). Averaged diurnal variation for the spring of 2010 (April,
268 May, and June) also showed that CH_4 absorption was weakened after precipitation (Fig. 6d).
269 Approximately a day after rainfall, CH_4 emission typically increased and/or absorption decreased (Fig. 5a,
270 b, e). The response of F_{CH_4} to rainfall was not obvious in winter (Figs. 5c and 6c).

271

272 **4. Discussion**

273 **4.1. Assignment of the REA system**

274 From comparison of CO₂ fluxes between the REA and EC data, we concluded that our REA system
275 generally provided a good approximation of the EC method and could thus be applied to measure F_{CH_4} .
276 One possible reason for the difference in CO₂ fluxes between the EC and REA methods is the method for
277 determining coefficient b in Eq. (1); coefficient b , although constant in Eq. 1, changes slightly and is not
278 constant throughout the day or year. Another possibility is that the loss of high frequency information due
279 to the switching speed of the REA valve system might lead to an underestimation of F_{CO_2} with the REA
280 method. However, the latter possibility was thought to be less likely because turbulent transfer was
281 significant at a lower frequency below 1 Hz at this site (Kosugi et al. 2007; Ueyama et al. 2009).

282 The most difficult part of measuring F_{CH_4} in the forest canopy is that the F_{CH_4} detection limit is very
283 close to the actual flux range. Although F_{CH_4} was larger than the detection limit in summer, fall, and
284 spring, it was smaller in winter. Chamber studies revealed that F_{CH_4} ranged from approximately 0 to 720
285 nmol m⁻² s⁻¹ in wetlands and from -1.7 to 1.4 nmol m⁻² s⁻¹ in water-unsaturated forest floors (Itoh et al.
286 2005, 2007, 2009); some of these values are smaller than the detection limit of our REA system. We
287 suggest that further improvements in measurement precision for the difference between upward and
288 downward air CH₄ concentration are required to measure F_{CH_4} more precisely particularly in the winter. A

289 possible approach to improving the precision of our REA system is to apply the hyperbolic REA method
290 (Bowling et al. 1999), which samples air only for high turbulent transport eddies. Applying this method
291 would allow us to increase the CH₄ concentration differences (up to a factor of 2.7; Bowling et al. 1999)
292 and thus improve the precision of the REA system. One disadvantage of the hyperbolic REA is that the
293 majority of air (80%) is discarded, and roughly 10% of the original volume is sampled into each of the
294 updraft and downdraft reservoirs (Bowling et al. 2003). The information contained in the discarded air
295 must be reconstructed through the coefficient *b*. The *b* is determined under the assumption of the scalar
296 similarity between temperature, CO₂ and CH₄, so under some conditions large errors can result from
297 violation of scalar similarity using the hyperbolic REA (Ruppert 2002).

298

299 **4.2. Amplitude and seasonal variations in CH₄ flux and its response to rainfall**

300 At the study site, the main CH₄ sources areas (riparian wetlands) were heterogeneously distributed
301 within the flux footprint area, as shown in Fig. 1, and the typical wind direction (described in Section 2.1)
302 did not change seasonally. Although there were large CH₄ sources in the north and south, daytime and
303 night-time F_{CH_4} from the north or south were not particularly larger than those from other wind directions
304 (Fig. 4). Although there was a difference between the F_{CH_4} from the north and south in summer 2010, this
305 was probably caused by artificial difference due to limited number of available data; F_{CH_4} in summer
306 2010 could not be affected by wind direction. Thus, we assumed that the observed F_{CH_4} seasonal

307 variations would be mainly caused by the activity of methanogens and methanotrophs influenced by the
308 soil temperature and water conditions but not wind direction.

309 Itoh et al. (2005, 2007, 2009) measured seasonal CH₄ flux variations from different parts of the slope
310 in a water-unsaturated forest floor and riparian wetlands at the study site using the chamber method from
311 2001 to 2005. They showed that CH₄ emission rates from wetlands ranged from 0 to 720 nmol m⁻² s⁻¹, and
312 that the emission rates increased significantly during high soil temperature and VSWC periods. They
313 hypothesised that the emission rates were large enough to turn the entire watershed into a net CH₄ source,
314 even though the source areas were very limited (Itoh et al. 2005). The emission rates from the wetlands
315 varied from year to year due to the hydrological conditions that changed in relation to precipitation
316 patterns (particularly summer precipitation patterns) (Itoh et al. 2007). The reported CH₄ fluxes from the
317 water-unsaturated forest floor at this site ranged from -1.7 to 1.4 nmol m⁻² s⁻¹ (Itoh et al. 2009). CH₄
318 uptake was usually observed throughout the sampling periods; however, on lower hillslopes, where
319 groundwater constantly existed underground, weak CH₄ uptake was observed only at low soil temperature
320 (< 15°C); these areas turned to a CH₄ source at high soil temperatures (Itoh et al. 2009). The chamber
321 measurements revealed that CH₄ fluxes in this forest were heterogeneous at both temporal and spatial
322 scales, thus highlighting the importance of conducting continuous measurements of canopy-scale CH₄
323 fluxes integrated over a larger area to evaluate the total CH₄ budget.

324 Four new insights were obtained by combining the results from earlier chamber studies and this study.

325 First, the canopy-scale F_{CH_4} results by the REA method showed emission in the summer and fall of 2009,
326 indicating that a forest ecosystem consisting mostly of a water-unsaturated forest floor could be a CH_4
327 source for an entire watershed, possibly due to a large source contribution by a tiny wetland (Whalen et al.
328 1990; Keller and Reiners 1994; Hudgens and Yavitt et al. 1997; Itoh et al. 2007). Another possible source
329 was the contribution from the lower hillslopes of the water-unsaturated forest floor. Even though the soil
330 surface was water-unsaturated, groundwater constantly existed underground and produced CH_4 under
331 anaerobic conditions, which could have been emitted (Itoh et al. 2009). This study shows, for an entire
332 watershed, that a Japanese cypress forest in a warm temperate climate could be a CH_4 source in summer
333 and fall according to tower based measurements. Previous chamber-based studies speculated on the
334 canopy-scale CH_4 dynamics from the plot-scale measurements, which might contain large uncertainties.
335 Our canopy-scale measurements support the results of earlier chamber measurements. We found that
336 monthly averaged F_{CH_4} in October of 2009 was $6.6 \text{ nmol m}^{-2} \text{ s}^{-1}$ and it was not far less than the average
337 CH_4 fluxes in a peat meadow ($29.7 \text{ nmol m}^{-2} \text{ s}^{-1}$, Hendriks et al. 2008), a dairy farm ($42.7 \text{ nmol m}^{-2} \text{ s}^{-1}$,
338 Kroon et al. 2007) and a boreal fen ($80 \text{ nmol m}^{-2} \text{ s}^{-1}$, Long et al. 2010). It is not negligible CH_4 emission
339 from forest ecosystems, and it is important to quantify CH_4 fluxes in forest ecosystems and monitor it in
340 the long-term.

341 Second, continuous measurements at high temporal resolution revealed that the canopy-scale CH_4
342 emissions increased and/or absorption decreased after rainfall particularly in summer and fall of 2009.

343 The F_{CH_4} response to rainfall was caused by changes in the soil water condition because the methanogenic
344 activities increase and methanotrophic activities decrease in anoxic environments (Le Mer and Roger
345 2001). The area of the CH_4 source was broadened along the riparian zones after rainfall, and the lower
346 hillslope part of the water-unsaturated forest floor may have switched from a sink to a source for CH_4
347 because the anaerobic area may also have broadened deep underground, as mentioned above. Another
348 possibility is that CH_4 diffusion from the air to the soil may have been inhibited by rainfall causing a
349 decline in CH_4 absorption (Bradford et al. 2001). As shown in Fig. 5a, b, e, the influence of rainfall to
350 F_{CH_4} was obvious 1 or 2 days after rainfall events, at the short time-scale. On the other hand, F_{CH_4} tended
351 to be influenced by rainfall in the seasonal time-scale as seen in the shift of F_{CH_4} to emission during
352 summer 2010 (Fig. 3a). F_{CH_4} seemed to shift from absorption to emission during about 2 weeks after
353 intense rainfalls in late July 2010 (Fig. 3a). These different time-scale responses of F_{CH_4} to rainfall were
354 probably caused by different processes, and should be investigated with more data. In winter, the
355 response of F_{CH_4} to rainfall appeared to be low, suggesting that less CH_4 was produced and/or absorbed in
356 winter compared to other seasons; the activities of both methanogens and methanotrophs are low at low
357 soil temperatures, although methanotrophs are much less temperature dependent (Dunfield et al. 1993).

358 Third, CH_4 absorption rates increased from spring 2010 as soil temperatures increased and VSWC
359 decreased. These results are consistent with previous chamber measurements (Itoh et al. 2009). Uptake
360 rates increased as soil temperature increased in the lower range of temperature ($<15^\circ\text{C}$) and as VSWC

361 decreased. Previous studies reported a similar activation of methanotrophs with an increase in
362 temperature (Whalen et al. 1990; Dobbie et al. 1996; Prime and Christensen 1997; Ishizuka et al. 2000).
363 In contrast, methanogens function at intermediate temperature ranges from 20 to 40°C (Yamane et al.
364 1961), and their activity is extremely low at low temperatures (Dunfield et al. 1993). The large F_{CH_4}
365 absorption obtained in the spring of 2010 by the REA method was possibly due to the different responses
366 of methanogens and methanotrophs to temperature. Methanotrophs might function well under conditions
367 where methanogens are still unable to function well (i.e., low temperature) (Dunfield et al. 1993; La Mer
368 and Roger 2001). We still do not have enough information to explain the differences in F_{CH_4} between fall
369 2009 and spring 2010 within a similar temperature range. These differences represent complex behaviour
370 beyond that expected on the basis of previous plot-scale measurements. The difference in temperature
371 before the sampling season (summer or winter in this case) might have affected both methanogenic and
372 methanotrophic activities during these periods. Longer duration observational data are needed to help
373 clarify the seasonal F_{CH_4} variation in forest ecosystems.

374 Finally, the CH_4 absorption rates in spring 2010 (monthly averaged F_{CH_4} from April to June of 2010
375 ranged from -5.1 to -18.3 $\text{nmol m}^{-2} \text{s}^{-1}$) were larger than those reported by the previous chamber study
376 (-1.7 to 1.4 $\text{nmol m}^{-2} \text{s}^{-1}$; Itoh et al. 2009) at the water-unsaturated forest floor at this site. Although the
377 CH_4 fluxes obtained by the REA and chamber measurements cannot be compared directly, one possible
378 explanation involves the detection limit of our REA system ($4.2 \pm 3.7 \text{ nmol m}^{-2} \text{ s}^{-1}$ in the night-time and

379 $7.4 \pm 5.9 \text{ nmol m}^{-2} \text{ s}^{-1}$ in the daytime), which may not be sufficient to detect the range of CH_4 uptake rates
380 obtained by the chamber method for the water-unsaturated forest floor (-1.7 to $1.4 \text{ nmol m}^{-2} \text{ s}^{-1}$). The
381 other possible reason is that the chamber method is not always an excellent tool for investigating
382 representative CH_4 flux over a large watershed. An unobserved area that is consuming CH_4 more
383 effectively than estimated previously might exist at the study site. Recently, we have been conducting
384 continuous chamber measurements of CH_4 flux using the same TDLS CH_4 analyzer at the
385 water-unsaturated forest floor at the study site and have found several times higher CH_4 absorption rates
386 than the earlier chamber measurements at one of three automated chambers (unpublished data). These
387 results suggest that canopy-scale measurements using micrometeorological methods are important to
388 evaluate total CH_4 exchange and its impact on the environment.

389

390 **Conclusions**

391 This study is the first report of continuous measurements of canopy-scale F_{CH_4} in an upland forest
392 using the REA method with a TDLS CH_4 analyzer. Our observations revealed how the entire forest
393 ecosystem complexly switched between being a CH_4 sink or a source on hourly, diurnal, and seasonal
394 scales. As micrometeorological methods provide spatially integrated fluxes with high temporal
395 resolutions, measuring F_{CH_4} with these methods is particularly important to investigate the CH_4 dynamics
396 in forest ecosystems. In this study, we demonstrated that the REA method is applicable for measuring

397 CH₄ flux over a large representative area. Further longer-term observations with improvement of the
398 system are needed to evaluate the controlling factors for methanogens and methanotrophs activity in the
399 CH₄ dynamics of forest ecosystems. A combined approach between conventional chamber and
400 micrometeorological methods is particularly important to evaluate the total CH₄ exchange, its impact on
401 the environment, and the detailed processes involved.

402

403 **Acknowledgements**

404 This work was supported in part by a Grant-in-Aid for Scientific Research from the Ministry of Education,
405 Culture, Sports, Science and Technology (MEXT) of Japan.

406

407 **Figure captions**

408 Figure 1 Topographic map of the observation site. Precipitation was recorded at the indicated
409 meteorological station. The streams are shown as bold lines, and riparian zones are located along
410 the streams. The main wetland areas are in black.

411 Figure 2 Comparison between CO₂ fluxes obtained by the REA and EC methods at the half-hourly time
412 scale in the **a** daytime (0600-1800 h) and **b** nighttime (0000-0600 and 1800-2400 h). The thin
413 and bold lines represent 1:1 and linear regression, respectively. The linear regression equation
414 and r^2 obtained from analysis of all data are shown.

415 Figure 3 Seasonal variation in **a** instantaneous canopy CH₄ flux and CH₄ flux assumed to be zero by the
416 *t*-test (grey circles), **b** air temperature and soil temperature (grey lines), and **c** precipitation and
417 the volumetric soil water content (VSWC) at the water-unsaturated forest floor during August
418 2009 and August 2010, in an evergreen Japanese cypress forest in a warm temperature climate.

419 Figure 4 Daytime and night-time CH₄ fluxes averaged for each wind direction (north, south, east, west) in
420 each season: **a** the sum of all seasons, **b** summer 2009, **c** fall 2009, **d** winter 2009, **e** spring 2010,
421 and **f** summer 2010 are shown. Daytime and night-time CH₄ fluxes are shown as white and
422 black circles. Error bars show the standard deviations. The data used for averaging seasonal CH₄
423 fluxes for each wind direction are shown as bars. The data for daytime and night-time are shown
424 as white and black bars, respectively.

425 Figure 5 Diurnal course of instantaneous canopy CH₄ flux and CH₄ flux assumed to be zero by the *t*-test
426 (grey circles), precipitation, and air temperature and soil temperature (dotted lines) measured in
427 **a** summer (between 5 September and 14 September 2009), **b** fall (between 25 October and 3
428 November 2009), **c** winter (between 4 December and 8 December 2009 and between 7 March
429 and 11 March 2010), **d** early spring (between 1 March and 5 March 2010), and **e** late spring
430 (between 21 May and 30 May 2010) in an evergreen Japanese cypress forest in a warm
431 temperature climate.

432 Figure 6 Diurnal variations of CH₄ fluxes before precipitation (black circle) and after precipitation (white

433 circle) (in case accumulated precipitation was more than 2 mm half hour⁻¹) and air temperature,
434 averaged for **a** the summer of 2009 (August and September), **b** the fall of 2009 (October and
435 November), **c** the winter of 2009 (December, February and March), and **d** the spring of 2010
436 (April, May and June). Before and after precipitation were discriminated according to
437 accumulated precipitation within 24 h was more than 2 mm half hour⁻¹ or not. Error bars show
438 the standard deviations for CH₄ fluxes.

439

440 **References**

- 441 Aubinet M, Grelle A., Ibrom A, Rannik U, Moncrieff J, Foken T, Kowalski AS, Martin PH, Berbigier P,
442 Bernhofer C, Clement R, Elbers J, Granier A, Grunwald T, Morgenstern K, Pilegaard K, Rebmann
443 C, Snijders W, Valentini R, Vesala T (2000) Estimates of the annual net carbon and water exchange
444 of forests: the EUROFLUX methodology. *Adv. Ecol. Res.* 30:113–175.
- 445 Baer DS, Paul JB, Gupta M, O’Keefe A. (2002) Sensitive absorption measurements in the near-infrared
446 region using off-axis integrated cavity-output spectroscopy. *Appl. Phys.* B75:261–265.
- 447 Bowling DR, Pataki DE., Ehleringer JR (2003) Critical evaluation of micrometeorological methods for
448 measuring ecosystem-atmosphere isotopic exchange of CO₂. *Agric. Meteorol.* 3118:1-21.
- 449 Bowling DR, Delany AC, Turnipseed AA, Baldocchi DD, Monson RK (1999) Modification of the
450 relaxed eddy accumulation technique to maximize measured scalar mixing ratio differences in

451 updrafts and downdrafts. *J. Geophys. Res.* 104:9121-9133.

452 Bowling DR, Turnipseed AA, Delany AC, Baldocchi DD, Greenberg JP, Monson RK (1998) The use of
453 relaxed eddy accumulation to measure biosphere-atmosphere exchange of isoprene and other
454 biological trace gases. *Oecologia.* 116:306-315.

455 Bradford MA, Ineson P, Wookey PA, Lappin-Scott HM (2001) Role of CH₄ oxidation, production and
456 transport in forest soil CH₄ flux. *Soil Biol. and Biochem.* 33:1625-1631.

457 Businger JA, Oncley SP (1990) Flux measurement with conditional sampling. *J. Atmos. Oceanic Technol.*
458 7:349-352.

459 Denmead OT (1994) Measuring fluxes of CH₄ and N₂O between agricultural systems and the atmosphere.
460 In: Peng S, Ingram KT, Neue H-U, Ziska LH (eds) *Climate change and rice.* International Rice
461 Research Institute, Manila, Philippines.

462 Dobbie KE, Smith KA, Christensen S, Degorska A, Orlanski P (1996) Effect of land use on the rate of
463 methane uptake by surface soils in Northern Europe. *Atmos., Environ.* 30:1005-1011.

464 Dunfield P, Knowles R, Dumont R, Moore TR (1993) Methane production and consumption in
465 temperate and subarctic peat soils: response to temperature and pH. *Soil Biol. Biochem.*
466 25:321-326.

467 Foken T, Wichura B (1996) Tools for quality assessment of surface-based flux measurements. *Agric. For.*
468 *Meteorol.* 78:83-105.

469 Hamotani K, Uchida Y, Monji N, Miyata A (1996) A system of the relaxed eddy accumulation method to
470 evaluate CO₂ flux over plant canopies. *J. Agric. Meteorol.* 52(2):135–139.

471 Hamotani K, Monji N, Yamaguchi K (2001) Development of a long-term CO₂ flux measurement system
472 using REA method with density correction. *J. Agric. Meteorol.* 57(2):93–99.

473 Hendriks DMD, Dolman AJ, van der Molen MK, van Huissteden J (2008) A compact and stable eddy
474 covariance set-up for methane measurements using off-axis integrated cavity output spectroscopy.
475 *Atmos. Chem. Phys.* 8:431–443.

476 Hudgens DE, Yavitt JB (1997) Land-use effects on soil methane and carbon dioxide fluxes in near Ithaca,
477 New York. *Ecoscience.* 4(2):214–222.

478 Ishizuka S, Sakata T, Ishizuka K (2000) Methane oxidation in Japanese forest soils. *Soil Biol. Biochem.*
479 32:769–777.

480 Itoh M, Ohte N, Katsuyama M, Koba K, Kawasaki M, Tani M (2005) Temporal and spatial variability of
481 methane flux in a temperate forest watershed. *J. Japan Soc. Hydrol. Water Resour.* 18:244–256. (in
482 Japanese with English abstract)

483 Itoh M, Ohte N, Koba K, Katsuyama M, Hayamizu K, Tani M (2007) Hydrologic effects on methane
484 dynamics in riparian wetlands in a temperate Forest catchment. *J. Geophys. Res.* 112(G1):G01019.

485 Itoh M, Ohte N, Koba K (2009) Methane flux characteristics in forest soils under an East Asian monsoon
486 climate. *Soil Biol. Biochem.* 41:388–395.

487 Keller M, Reiners WA (1994) Soil-atmosphere exchange of nitrous oxide, nitric oxide, and methane
488 under secondary succession of pasture to forest in the Atlantic lowlands of Costa Rica. *Global*
489 *Biogeochem. Cycles*. 8(4):99-409.

490 Kim J, Verma SB, Billesbach DP (1998a) Seasonal variation in methane emission from a temperate
491 Phragmites-dominated marsh: effect of growth stage and plant-mediated transport. *Global Change*
492 *Biol*. 5:433–440.

493 Kim J, Verma SB, Billesbach DP, Clement RJ (1998b) Diel variation in methane emission from a
494 midlatitude prairie wetland: significance of convective throughflow in *Phragmites australis*. *J.*
495 *Geophys. Res.* 103:28,029–28,039.

496 Kosugi Y, Katsuyama M (2007) Evapotranspiration over a Japanese cypress forest. II. Comparison of the
497 eddy covariance and water budget methods. *J. Hydrol.*, 334:305–311.

498 Kosugi Y, Takanashi S, Tanaka H, Ohkubo S, Tani M, Yano M, Katayama T (2007) Evapotranspiration
499 over a Japanese cypress forest. I. Eddy covariance fluxes and surface conductance characteristics
500 for 3 years. *J. Hydrol.* 337:269–283.

501 Kroon PS, Hensen A, Jonker HJJ, Zahniser MS, van't Veen WH, Vermeulen AT (2007) Suitability of
502 quantum cascade laser spectroscopy for CH₄ and N₂O eddy covariance flux measurements.
503 *Biogeosciences*. 4:715-728.

504 LeMer J, Roger P (2001) Production, oxidation, emission and consumption of methane by soils: a review.

- 505 Eur. J. of Soil Biol. 37:25–50.
- 506 Long KD, Franagan LB, Cai T (2010) Diurnal and seasonal variation in methane emissions in a northern
507 Canadian peatland measured by eddy covariance. *Global Change Biol.* 16:2420–2435.
- 508 McDermitt D, Burba G, Xu L, Anderson T, Komissarov A, Riensche B, Schedlbauer J, Starr G, Zona D,
509 Oechel W, Oberbauer S, Hastings S (2011) A new low-power, open-path instrument for measuring
510 methane flux by eddy covariance. *Appl Phys. B*102:391-405.
- 511 McMillen RT, (1988) An eddy correlation technique with extended applicability to non-simple terrain.
512 *Boundary-Layer Meteorol.* 43:231–245.
- 513 Ohkubo S, Kosugi Y (2007) Amplitude and seasonality of storage fluxes for CO₂, heat and water vapor in
514 a temperate Japanese cypress forest. *Tellus.* 60B:11–20.
- 515 Ohkubo S, Kosugi Y, Takanashi S, Mitani T, Tani M (2007) Comparison of the eddy covariance and
516 automated closed chamber methods for evaluating nocturnal CO₂ exchange in a Japanese cypress
517 forest. *Agric. For. Meteorol.* 142:50–65.
- 518 Prime A, Christensen S (1997) Seasonal and spatial variation of methane oxidation in a Danish spruce
519 forest. *Soil Biol. Biochem.* 29:1165-1172.
- 520 Ruppert J (2002) Eddy sampling methods for the measurement of trace gas fluxes, Diploma thesis, 95pp,
521 University of Bayreuth.
- 522 Savage K, Moore TR, Crill PM (1997) Methane and carbon dioxide exchanges between the atmosphere

523 and northern boreal forest soils. *J. Geophys. Res.* 102:29279–29288.

524 Schrier-Uijl AP, Veenendaal EM, Leffelaar PA, van Huissteden JC, Berendse F (2009) Methane
525 emissions in two drained peat agro-ecosystems with high and low agricultural intensity. *Plant Soil.*
526 doi:10.1007/s11104-009-0180-1.

527 Schuepp PH, Leclerc MY, MacPherson JJ, Desjardins RL (1990) Footprint prediction of scalar fluxes
528 from analytical solutions of the diffusion equation. *Boundary-Layer Meteorol.* 50:335–373.

529 Silver WL, Lugo AE, Keller M (1999) Soil oxygen availability and biogeochemistry along rainfall and
530 topographic gradients in upland wet tropical forests soil. *Biogeochemistry.* 44:301–328.

531 Simpson IJ, Thurtell GW, Kidd GE, Lin M, Demetriades-Shah TH, Flitcroft ID, Kanemasu ET, Nie D,
532 Bronson KF, Neue HU (1994) Tunable diode laser measurements of methane fluxes from an
533 irrigated rice paddy field in the Philippines. *J. Geophys. Res.* 100:7283–7290.

534 Smeets CJPP, Holzinger R, Vigano I, Goldstein AH, Röckmann T (2009) Eddy covariance methane
535 measurements at a Ponderosa pine plantation in California. *Atmos. Chem. Phys.* 9:8365–8375.

536 Takanashi S, Kosugi Y, Tanaka Y, Yano M, Katayama T, Tanaka H, Tani M (2005) CO₂ exchange in a
537 temperate Japanese cypress forest compared to that in a cool-temperate deciduous broadleaved
538 forest. *Ecol. Res.* 20:313–324.

539 Ueyama M, Hamotani K, Nishimura W (2009) A technique for high-accuracy flux measurement using a
540 relaxed eddy accumulation system with an appropriate averaging strategy. *J. Agric. Meteorol.*

541 65(4):315–325.

542 Van den Pol-van Dasselaar A, Van Beusichem ML, Oenema O (1998) Effects of soil moisture content
543 and temperature on methane uptake by grasslands on sandy soils. *Plant Soil*. 204:213-222.

544 Wang FL, Bettany JR (1997) Methane emission from Canadian prairie and forest soils under short term
545 flooding conditions. *Nutr. Cycling Agroecosyst*. 49:197–202.

546 Webb EK, Pearman GI, Leuning R (1980) Correction of flux measurements for density effects due to heat
547 and water vapour transfer. *Q., J. R. Meteorol*. 106:85–100.

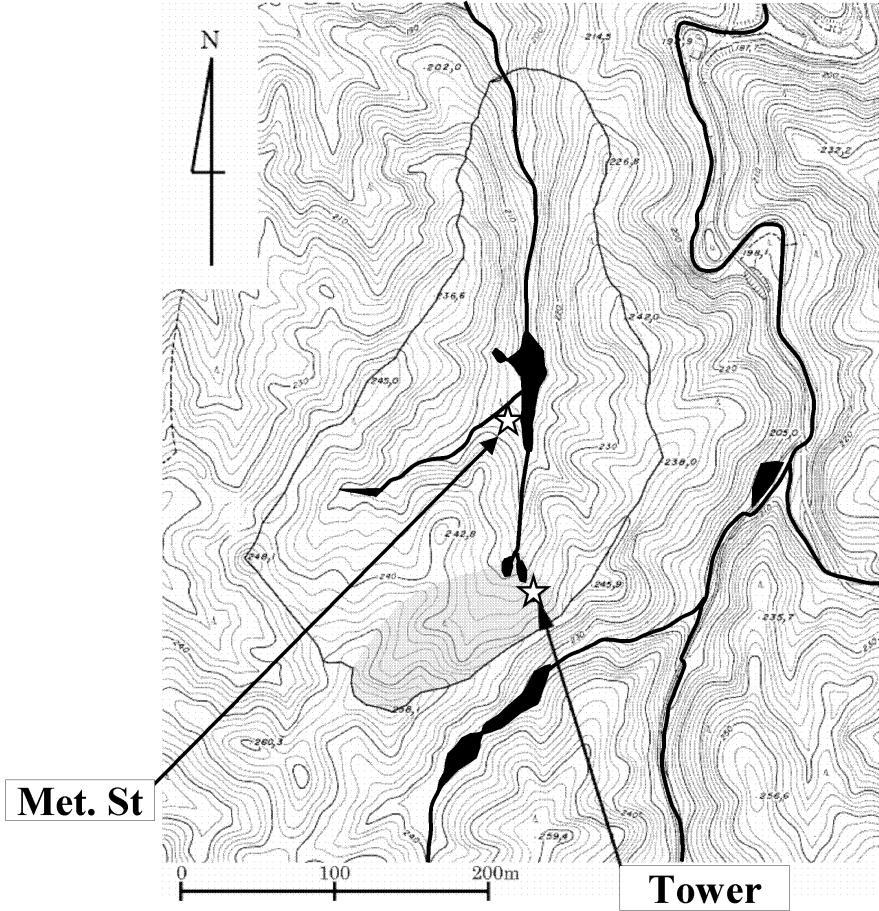
548 Whalen SC, Reeburgh WS, Sandbeck KA (1990) Rapid methane oxidation in a landfill cover soil. *Appl*
549 *Environ Microbiol*. 56(11):3405-3411.

550 Yamane I, Sato K (1961) Effect of temperature on the formation of gases and ammonium nitrogen in the
551 water-logged soils. *Sci. Rep. Res. Inst. Tohoku Univ. D(Agr)*. 12:31-46.

552

553 The English in this document has been checked by at least two professional editors, both native speakers of
554 English. For a certificate, please see:
555
556 <http://www.textcheck.com/certificate/pm8wW1>
557
558

559 Figure 1



560

561

562

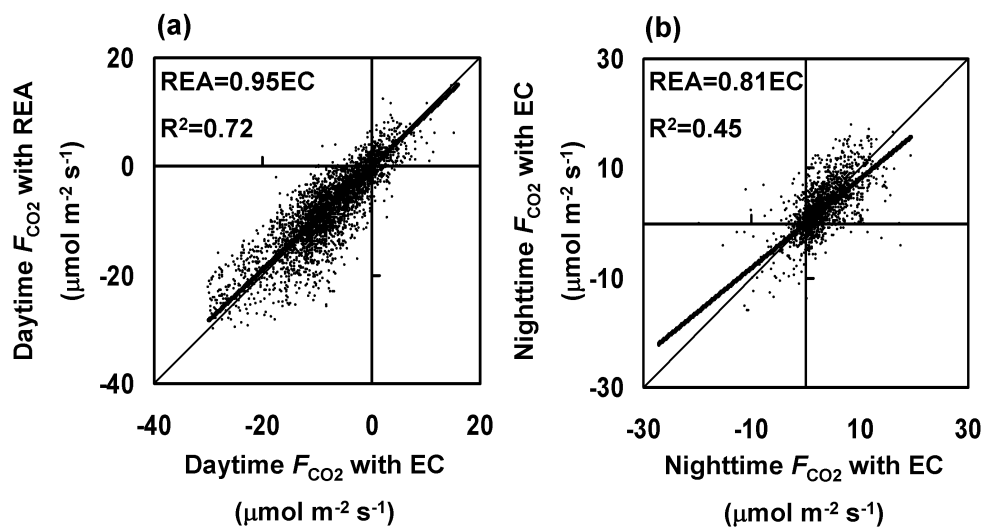
563

564

565

566

567



569

570

571

572

573

574

575

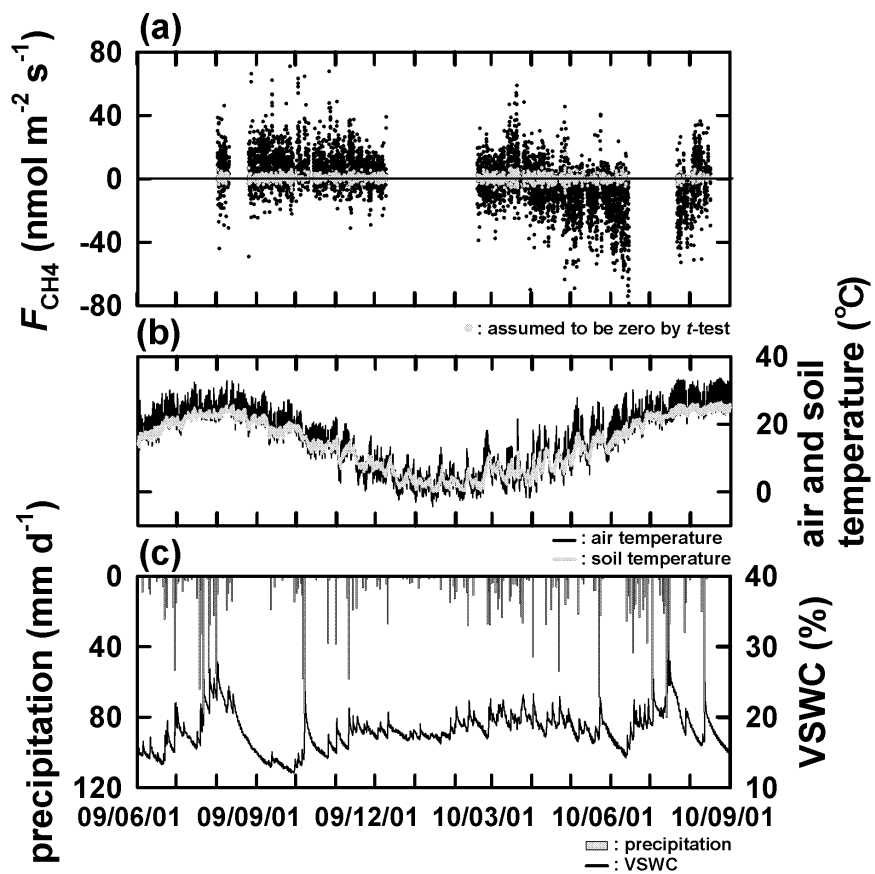
576

577

578

579

580



582

583

584

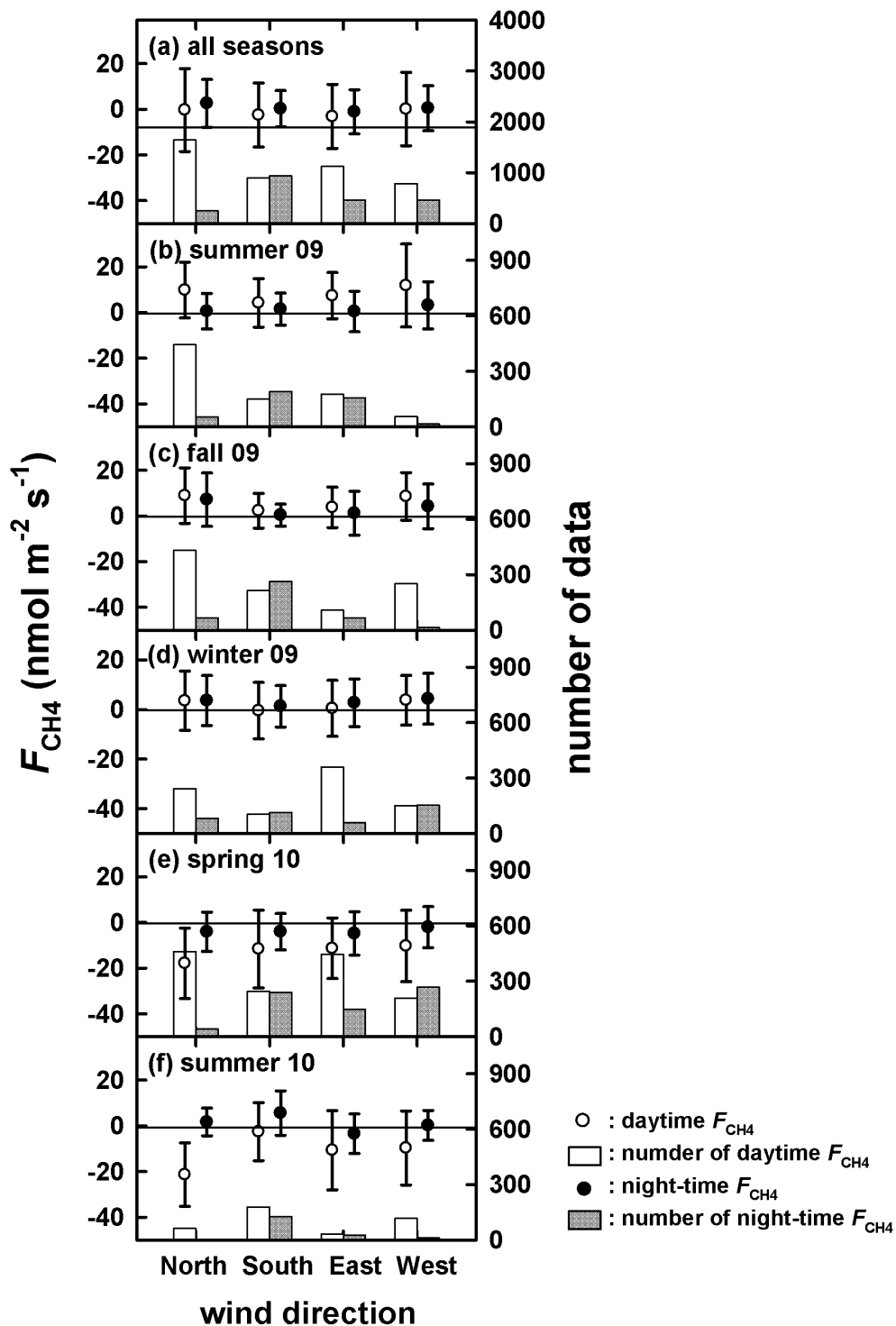
585

586

587

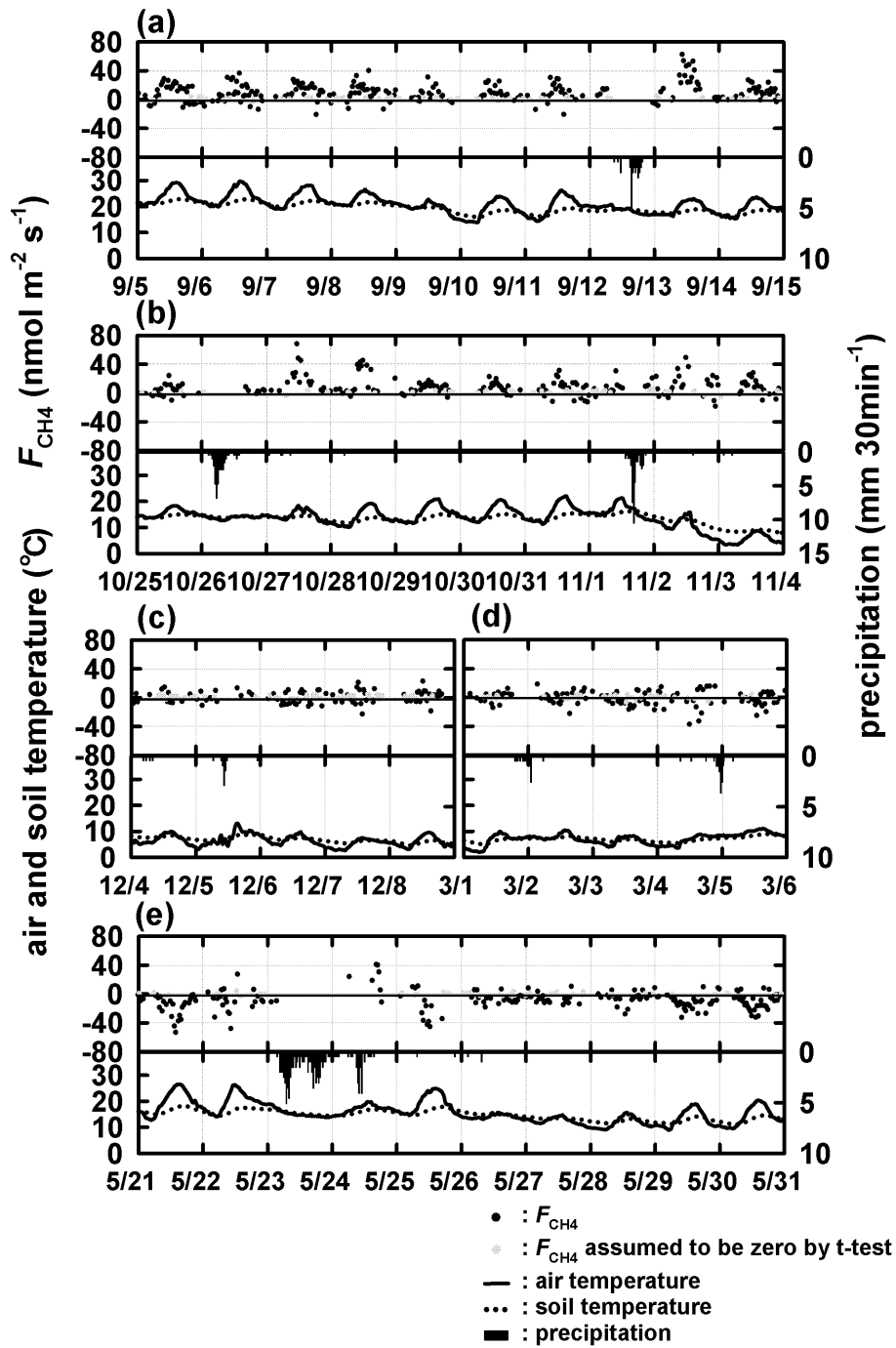
588

589



591

592



594

595

596

